frontiers in
HUMAN NEUROSCIENCE

IMPACT 2.9 FACTOR

# MicroRNA-138 is a potential regulator of memory performance in humans

Julia Schröder, Sara Ansaloni, Marcel Schilling, Tian Liu, Josefine Radke, Marian Jädicke, Brit-Maren M Schjeide, Andriy Mashychev, Christina Tegeler, Helena Radbruch, Goran Papenberg, Sandra Düzel, Ilja Demuth, Nina Bucholtz, Ulman Lindenberger, Shu-Chen Li, Elisabeth Steinhagen-Thiessen, Christina M Lill and Lars Bertram

| | |
|---|---|
| Journal Name: | Frontiers in Human Neuroscience |
| ISSN: | 1662-5161 |
| Article type: | Original Research Article |
| Received on: | 15 Apr 2014 |
| Accepted on: | 20 Jun 2014 |
| Provisional PDF published on: | 20 Jun 2014 |
| www.frontiersin.org: | www.frontiersin.org |
| Citation: | Schröder J, Ansaloni S, Schilling M, Liu T, Radke J, Jädicke M, Schjeide BM, Mashychev A, Tegeler C, Radbruch H, Papenberg G, Düzel S, Demuth I, Bucholtz N, Lindenberger U, Li S, Steinhagen-thiessen E, Lill CM and Bertram L(2014) MicroRNA-138 is a potential regulator of memory performance in humans. *Front. Hum. Neurosci.* 8:501. doi:10.3389/fnhum.2014.00501 |
| /Journal/Abstract.aspx?s=537&name=human%20neuroscience&ART_DOI=10.3389/fnhum.2014.00501: | /Journal/Abstract.aspx?s=537&name=human%20neuroscience&ART_DOI=10.3389/fnhum.2014.00501 |
| | (If clicking on the link doesn't work, try copying and pasting it into your browser.) |

# MicroRNA-138 is a potential regulator of memory performance in humans

Julia Schröder[1,2], Sara Ansaloni[1], Marcel Schilling[1,3], Tian Liu[1,4], Josefine Radke[5], Marian Jaedicke[1], Brit-Maren M. Schjeide[1], Andriy Mashychev[1], Christina Tegeler[2], Helena Radbruch[5], Goran Papenberg[4,6], Sandra Düzel[4], Ilja Demuth[2,7], Nina Bucholtz[2], Ulman Lindenberger[4], Shu-Chen Li[4,8], Elisabeth Steinhagen-Thiessen[2], Christina M. Lill[1,9], Lars Bertram[1,10*]

[1]Department of Vertebrate Genomics, Max Planck Institute for Molecular Genetics. Berlin, Germany
[2]Charité Research Group on Geriatrics, Charité – Universitätsmedizin Berlin, Berlin, Germany
[3]Berlin Institute for Medical Systems Biology, Max Delbrück Center for Molecular Medicine, Berlin, Germany
[4]Center for Lifespan Psychology, Max Planck Institute for Human Development, Berlin, Germany
[5]Department of Neuropathology, Charité – Universitätsmedizin Berlin, Berlin, Germany
[6]Aging Research Center, Karolinska Institute, Stockholm, Sweden
[7]Institute of Medical and Human Genetics, Charité – Universitätsmedizin Berlin, Berlin, Germany
[8]Department of Psychology, Lifespan Developmental Neuroscience, TU Dresden, Dresden, Germany
[9]Department of Neurology, Focus Program Translational Neuroscience, University Medical Center of the Johannes Gutenberg University Mainz, Mainz, Germany
[10]School of Public Health, Faculty of Medicine, Imperial College London, London, UK

*Correspondence:

Lars Bertram
Neuropsychiatric Genetics Group
Department of Vertebrate Genomics,
Max Planck Institute for Molecular Genetics
Ihnestraße 63-73, D-14195 Berlin, Germany
(T) +49-30-8413-1876 (F) +49-30-8413-1139
(E) lbertram@molgen.mpg.de

**Keywords:** genome-wide association study, GWAS, working memory, episodic memory, microRNA, hsa-mir-138-5p, *DCP1B*

**Abstract**

Genetic factors underlie a substantial proportion of individual differences in cognitive functions in humans, including processes related to episodic and working memory. While genetic association studies have proposed several candidate "memory genes", these currently explain only a minor fraction of the phenotypic variance ~~suggesting that additional genetic factors are involved~~. Here, we performed genome-wide screening on 13 episodic and working memory phenotypes in ~~up to~~ 1,318 participants of the Berlin Aging Study II ~~(BASE-II)~~ aged 60 years or older. The analyses highlight a number of novel single nucleotide polymorphisms (SNPs) associated with memory performance, including one ~~marker~~ located in a putative regulatory region of microRNA (miRNA) hsa-mir-138-5p (rs9882688, P-value = $7.8 \times 10^{-9}$). Expression quantitative trait locus analyses on next-generation RNA-sequencing data revealed that rs9882688 genotypes show a significant correlation with the expression levels of this miRNA in 309 human lymphoblastoid cell lines (P-value = $5 \times 10^{-4}$). *In silico* modeling of other top-ranking GWAS signals identified an additional memory-associated SNP in the 3' untranslated region (3'UTR) of *DCP1B*, a gene encoding a core component of the mRNA decapping complex in humans, predicted to interfere with hsa-mir-138-5p binding. This prediction was confirmed *in vitro* by luciferase assays showing differential binding of hsa-mir-138-5p to 3'UTR reporter constructs in two human cell lines (HEK293: P-value = 0.0470; SH-SY5Y: P-value = 0.0866). Finally, expression profiling of hsa-mir-138-5p and *DCP1B* mRNA in human post-mortem brain tissue revealed that both molecules are expressed simultaneously in frontal cortex and hippocampus, suggesting that the proposed interaction between hsa-mir-138-5p and *DCP1B* may also take place *in vivo*. In summary, by combining unbiased genome-wide screening with extensive *in silico* modeling, *in vitro* functional assays, and gene expression profiling, our study identified miRNA-138 as a potential molecular regulator of human memory function.

## 1. Introduction

Interindividual variations of memory performance in humans are regulated by genetic and non-genetic factors. Early estimates from twin studies suggest that approximately half of the phenotypic variance is attributable to heritable factors, while the remainder reflects shared and non-shared environmental factors (McClearn *et al.* 1997). These estimates have since received broad support from studies using different designs and analysis approaches (for recent review see Goldberg Hermo *et al.* 2014). For measures of general cognitive ability, the presumed genetic effects appear to increase across the lifespan, that is, from childhood to adulthood and late life (McClearn *et al.* 1997), suggesting that searching for genes in this domain may be most powerful in data sets of aged individuals (see also Lindenberger *et al*. 2008).

A number of candidate genes that may affect various aspects of memory performance in humans have been proposed to date (for review see Papassotiropoulos and de Quervain 2011). As is the case for many other genetically complex traits in humans, the most convincing of these have only recently emerged in the context of genome-wide association studies (GWAS; see NHGRI's "GWAS catalog" for an up-to-date overview; URL: http://www.genome.gov/gwastudies/; Welter *et al.* 2014). Among the most prominent findings are common polymorphisms (i.e. single nucleotide polymorphisms [SNPs]) in *WWC1* (WW and C2 containing 1, a.k.a. *KIBRA* for kidney and brain expressed protein; Papassotiropoulos *et al.* 2006) and *CTNNBL1* (catenin, beta like 1). *WWC1* is located on chromosome (chr) 5q34 and was identified nearly a decade ago in a GWAS on episodic memory in ~300 subjects in which the lead SNP (rs17070145) showed evidence for genome-wide significant association (Papassotiropoulos *et al.* 2006). Since the original study, a number of follow-up studies have been published, albeit with mixed results (Milnik *et al.* 2012). The other lead "memory gene", *CTNNBL1* (located on chr 20q11.23) was identified by the same group in a more recent GWAS (Papassotiropoulos and de Quervain 2011). Thus far, no reports have been published confirming this latter finding independently. In addition, a number of other candidate genes have been tested in non-GWAS association studies, some suggesting evidence for an increased effect sizes when comparing older vs. younger adults (Li *et al.* 2013; Papenberg *et al.* 2014).

A second – and thus far largely independent – line of genetic experiments suggests that memory performance, and likely a large number of other cognitive domains, may be influenced by the action of microRNAs (miRNAs). MiRNAs are short (i.e. typically between 18 and 24 nucleotide long), non-coding RNA molecules that are involved in regulating protein expression post-transcriptionally. This is achieved by binding to the target messenger-RNAs (mRNAs), thereby directly or indirectly interfering with mRNA translation. The last decade of research has shown that miRNAs are involved in a broad range of cellular functions, including the development, differentiation, proliferation, apoptosis, and metabolism of neurons and many other cell types in humans (Satoh 2012). Some estimates suggest that the expression of up to 50% of all human proteins may be affected by the action of one or more of the >2500 miRNAs currently believed to exist (URL: http://mirbase.org/index.shtml; Griffiths-Jones *et al.* 2006). One important factor determining the extent of miRNA-mediated expressional regulation is the binding affinity between miRNAs and their target mRNAs. This

is largely influenced by sequence complementarity between the respective interacting regions on both molecules (Peterson *et al.* 2014). Naturally occurring DNA sequence variants, e.g. trait associated SNPs, within the binding domains of either of these interactants can thus be expected to interfere with miRNA-to-mRNA binding either by decreasing (disruption of complementary sites) or increasing (creation of complementary sites) binding affinity.

In this study, we specifically searched for memory-associated DNA sequence variants predicted to affect miRNA-to-mRNA binding using a similar strategy as described previously by our group (Lill *et al.* 2014). Genetic associations, with measures of both working and episodic memory functions were assessed via genome-wide screening as part of an ongoing GWAS in participants of the Berlin Aging Study II (BASE-II). Associated SNPs were evaluated for their potential effects on miRNA-to-mRNA binding *in silico* using a bioinformatic prediction tool developed by our group. SNPs showing association with memory performance and predicted to directly alter miRNA-to-mRNA binding were further followed up using a range of *in vitro* experiments involving luciferase reporter assays in two human cell lines, as well as miRNA and mRNA expression profiling in human brain autopsy material from three adult individuals. Our analyses uncovered three memory-associated SNPs which potentially manifest their molecular effects by interfering with miRNA function. Intriguingly, two of these SNPs, by independent mechanisms, affect hsa-mir-138-1, a miRNA long known to be crucial in CNS development and function in mammals (Miska *et al.* 2004, Siegel *et al.* 2009) but hitherto not specifically linked to cognitive performance in humans.

## 2. Methods

### 2.1. Genome-wide association study (GWAS) of episodic and working memory performance in humans.

*Participants.* All GWAS participants were part of the Berlin Aging Study II (BASE-II), a multidisciplinary project investigating factors involved in 'healthy' vs. 'unhealthy' aging (Bertram *et al.* 2013). In addition to genetics, BASE-II covers a broad range of functional domains critical for understanding aging investigated in a multidisciplinary assessment protocol that includes measures from internal medicine, immunology, psychology, as well as sociology and economics. The behavioral test battery applied to each BASE-II participant includes an extensive coverage of cognitive abilities, including detailed assessments of working and episodic memory. At baseline, BASE-II includes 2,200 participants of Caucasian ancestry recruited from the greater Berlin area. The cohort is split into a subgroup of 1,600 older adults aged 60 to 80 years, mean 66.76 years at baseline, and 600 younger adults aged 20 to 35 years, mean 27.32 years. Both groups consist of equal numbers of males and females. The analyses presented here are limited to participants of the "old" stratum for whom genotype and cognitive data were available at the time of analysis (n = 1,318). Written consent was provided by all BASE-II individuals before participation. The study was approved by the institutional review boards of each relevant participating research unit prior to participant recruitment.

*Assessment of memory performance.* This study is based on 13 different quantitative measures (i.e., 2 and 11 respectively) of working memory (WM) and episodic memory (EM) were selected, assessed either at the Center for Lifespan Psychology at the Max Planck Institute for Human Development (MPIHD; n = 1,318 individuals with cognitive testing completed at time of analysis) or at the Charité Research Group on Geriatrics (CRGG; n = 961 with cognitive testing completed at time of analysis) at Charité University Hospital. At MPIHD, six participants from the same age group were tested simultaneously in two separate group sessions one week apart. In addition, we utilized test results from the CERAD Plus battery (Morris *et al.* 1989; Fillenbaum *et al.* 2008,), which was carried out individually to each participant at CRGG. See Supplementary Table 1 and Supplementary Methods for more detailed information on the type of WM and EM assessments used here.

*Genotyping and genetic association analyses.* Details on genotyping and analysis procedures can be found in the Supplementary Methods. In brief, DNA from all BASE-II participants was extracted from whole blood using standard procedures and then subjected to microarray-based SNP genotyping using the "Genome-Wide Human SNP Array 6.0" (Affymetrix, Inc.), followed by an extensive quality control and genome-wide imputation of unobserved genotypes using whole genome sequence data from the 1000 Genomes Project (Abecasis *et al.* 2010). Association analyses were carried out using the EM or WM variables as quantitative traits assuming an additive linear model, adjusted for age, sex, and years of education and to the first three principal components to account for potential population stratification. Association analyses were performed using SNPTEST v.1.3 (Marchini and Howie 2010), which accounts for uncertainty of imputed genotype calls via missing data likelihood tests. Overall, in this study we tested a total of 12,607,232 high-quality SNPs for

genetic association with the memory traits in 1,318 (MPIHD) and 961 (CRGG) subjects from the BASE-II subgroup aged 60-80 years.

**2.2. *In silico* predictions of miRNA-to-mRNA binding and potential SNP effects.**

To systematically assess the potential impact of SNP allele-status on miRNA-to-mRNA binding, we utilized a bioinformatic tool recently developed by our group described in detail elsewhere (Schilling 2011, Schilling 2013). In brief, this entailed a prediction of potential miRNA binding sites for 3'UTRs of all known protein-coding transcripts (downloaded from Ensembl Genes 71, http://www.ensembl.org/biomart/martview) using miRanda v.3.38, TargetScan 5.09 and PITA and v19 of the mirBASE database (http://www.mirbase.org). Only SNPs displaying strong linkage disequilibrium (LD; i.e. $r^2$ of 0.8; estimated from whole genome sequence data of the 1000 Genomes phase 1 CEU reference panel; Abecasis *et al.* 2010) with GWAS SNPs were considered further. For these SNPs, we finally estimated the potential effects on miRNA-to-mRNA binding using a modified version of the support vector regression (SVR) method developed by Betel (Betel *et al.* 2010).

**2.3. *In vitro* assessment of SNPs predicted to affect miRNA-to-mRNA binding.**

*Cell culture and construct transfection.* Experiments were performed as previously described (Lill *et al.* 2014). Custom made reporter plasmids (pLightSwitch_3UTR) containing the appropriate 3'UTR sequence and the miRNA mimics were purchased from SwitchGear Genomics (Menlo Park, CA, USA). The desired 3'UTRs were subcloned in the pLightSwitch_3UTR vector downstream of the *Renilla* luciferase gene. The UTR constructs containing the reference allele were used as a template to generate point mutations via site directed mutagenesis. All constructs were verified by Sanger sequencing. 3'UTR constructs were transfected into naïve human embryonic kidney (HEK293) and human neuroblastoma (SH-SY5Y) cells, which were cultured in DMEM GlutaMax (Invitrogen, Darmstadt, Germany) media with 10% FBS (Biochrom, Berlin, Germany) for HEK293 or 15% FBS for SH-SY5Y cells, with an additional 1% Penicillin/Streptomycin (Biochrom). The cells were grown in standard conditions (37°C, 5% $CO_2$). Transfection was carried out in 96-well plates (TPP, Trasadingen, Switzerland) at a cell confluency of about 50% using Dharmafect (ThermoScientific) following manufacturer´s instructions. 50ng of vector with the desired 3'UTR and 50nM of corresponding miRNA mimic or scrambled non-binding miRNA were co-transfected in the cells per well. The scrambled miRNA was used as a negative control in combination with all 3'UTR constructs and in all experiments. After 24 hours, HEK293 and SH-SY5Y cells were collected by freezing the culture plates directly on dry ice to enhance cell lysis. The plates were then thawed on ice and the resuspended cell lysates used for the luciferase assays. The LightSwitch Assay reagents (SwitchGear Genomics) were used following manufacturer´s instructions. Assay reagents mixed with the same volume of cell lysate were transferred to a white 96-well plate (Costar, Washington, D.C., USA). An end point read of *Renilla* luciferase intensity values was taken using the POLARStar Omega (BMG Labtech, Ortenburg, Germany) plate reader with three seconds integration time and 3,500 gain per well. Five to seven independent experiments per cell line and experimental condition were performed, using independent transfection mixes and/or different cell batches. For each independent experiment, six replicates were performed.

*Statistical analysis of luciferase data.* The analysis of the luciferase assay results were performed using R, an open-source language and environment for statistical computing and graphic (URL: http://www.r-project.org). We observed no outliers defined as deviating more than three standard deviations from the mean luciferase luminescence per experimental condition in each independent experiment. For each independent experiment, the mean luciferase activity of the 3'UTR reporter construct (i.e. containing either the reference or the alternative allele) co-transfected with a functional miRNA was divided by the baseline mean luciferase activity of the corresponding reporter construct co-transfected with the scrambled, non-targeting miRNA as negative control. To assess binding of the miRNAs to their predicted target sites irrespective of allele status, normalized luciferase activity of either 3'UTR reporter construct (i.e. either containing the reference or the alternative allele) co-transfected with the functional miRNA was compared to the control condition using the non-binding miRNA by one-sample t test (P-values reported for this analysis are one-tailed). Changes in *Renilla* gene expression levels in 3'UTR constructs containing the reference vs. alternative alleles were assessed based on the t test statistic for two independent samples (P-values reported for this analysis are two-tailed).

## 2.4. Analysis of expression levels of miRNA and mRNA molecules in human post-mortem brain tissue.

*Tissue preparation and RNA extraction.* Human brain tissue was collected post-mortem from hippocampi and frontal cortices from three deceased individuals without history of neuropsychiatric diseases at the Charité university hospital (Berlin, Germany). After collection, brain samples were stored (at -20°C) in RNA*later*® solution (Applied Biosystems, Forster City, CA, USA) to avoid degradation. We used the miRVANA™ miRNA Isolation Kit (Life Technologies, Darmstadt, Germany) to extract small and total RNAs from tissue samples following manufacturer´s instructions. Prior to extraction, all samples were homogenized using TissueLyser (QIAgen, Hilden, Germany) by shaking each sample twice in Lysis/Binding buffer for two minutes at 20Hz.

*Assessment of miRNA expression levels.* The quantification procedure comprises two steps: reverse transcription from RNA to cDNA followed by the amplification via quantitative PCR (qPCR). Specific primers for reverse transcription and qPCR were based on pre-made TaqMan® Small RNA Assays (Applied Biosystems). Reverse transcription was performed on 10ng RNA using the Taqman® MiRNA Reverse Transcription Kit according to the manufacturer's protocol (Applied Biosystems). The qPCR reaction was conducted using TaqMan® Small RNA Assays following the manufacturer's protocol (Applied Biosystems). In short this entailed: For reverse transcription 10ng of the extracted RNA was used in a reaction mix containing Reverse Transcription Buffer, 15mM dNTPs, 50U/µl MultiScribe™ Reverse Transcriptase, 20U/µl RNase Inhibitor, and Primer in a final volume of 15µl. The protocol in 384-well format for all reactions was as follows: 16°C for 30 min, 30 min at 42°C and a final step of 85°C for 5 min. The qPCR reaction was conducted in TaqMan® Universal PCR Master Mix II, TaqMan® Small RNA Assay (both Applied Biosystems) and 1.33µl of the RT-PCR product in a final volume of 20µl. The cycling protocol was: 10 min at 95°C, 15 sec at 95°C, 60 sec at 60°C for overall 50 cycles. The reactions were run and visualized on a QuantStudio™ 12K Flex Real-Time PCR System (Applied Biosystems).

*Assessment of mRNA expression levels.* Reverse transcription was performed using the High Capacity RNA-to-cDNA Kit (Applied Biosystems) on 0.2µg of total RNA following the manufacturer´s instructions. The reactions were run on the Thermo Cycler PTC-240 (MJ Research, Waltham, MA, USA). Expression of the resulting *DCP1B* cDNA was assessed via PCR primers 5'-CCAGGGTCTCCTCACAACAT-3' (forward) and 5'-TCTTTTTCATGGCTGCTTGA-3' (reverse). Primers were designed to lead to a ~850bp cDNA amplicon vs. a 6.9kb gDNA amplicon. PCR conditions were using 1.5µM of each primer, approximately 60ng of cDNA template, 0.25nM dNTPs, 10mM $MgCl_2$, 30% Q solution (QIAgen) and 0.25U Taq polymerase in a final volume of 10µl. Reactions were carried out in 96-well format on PTC-240 thermal cyclers at 94°C (3 min), followed by 40 cycles of 94°C (45 sec), 60.5°C (90 sec), and 72°C (60 sec), and a final extension step of 72°C (6 min). PCR amplicons were visualized by ethidium bromide stained gel electrophoresis in 1% agarose (Sigma Aldrich, Taufkirchen, Germany).

**2.5. Expression quantitative trait locus (eQTL) analyses of hsa-mir-138-5p using next-generation sequencing data.**

eQTL analyses on the potential role of rs9882688 in expression of hsa-miR-138-5p were performed using next-generation small RNA sequencing data of peripheral lymphoblastoid cell line (LCL) samples generated by the Genetic European Variation in Health and Disease (GEUVADIS) consortium (for a description of sequencing methods and data preparation see: Lappalainen *et al.* 2013). For the eQTL analyses here, we downloaded normalized expression data of hsa-miR-138-5p for four populations of European descent (i.e. Utah Residents with Northern and Western European Ancestry (CEU), Finns (FIN), British (GBR), Toscani (TSI)) as released by the GEUVADIS project database (URL: http://www.ebi.ac.uk/arrayexpress/files/E-GEUV-2/GD452.MirnaQuantCount.1.2N.50FN.samplename.resk10.txt). Subject-level genotypes for rs9882688 in the same individuals were obtained from the 1000 Genomes database (URL: http://browser.1000genomes.org/index.html; Abecasis *et al.* 2010). The resulting data set included 333 individuals of European descent with both hsa-miR-138-5p expression data and rs9882688 genotypes. Statistical analyses of these data were performed using R. MiRNA expression values that fell 1.5x the interquartile range (IQR) below the first quartile or 1.5x the IQR above the third quartile were defined as outliers and excluded from further analysis (24 samples). Expression levels of hsa-miR-138-5p showed a symmetrical, approximately normal distribution in the effective sample size of 309 individuals (as determined by the Shapiro-Wilk test implemented in R [P = 0.548] and quantile-quantile plotting, Suppl. Figure 1). Subsequent eQTL analyses on these 309 samples were based on an additive model using linear regression. Association results were adjusted for sex and population of origin. Due to the low frequency of homozygote carriers of the G allele (n = 2), sensitivity analyses were performed upon exclusion of those individuals. Statistical significance for these analyses is expressed as two-tailed P-values.

## 3. Results

### 3.1. GWAS of episodic and working memory performance in humans.

The GWAS analyses on 13 episodic and working memory traits in up to 1,318 individuals from the subgroup of BASE-II participants aged 60 years or older revealed 28 distinct genomic regions (or: loci) showing association P-values at $1x10^{-6}$ or below (Supplementary Table 2), indicating that at least some of these are genetically linked to human memory performance. Notably, these did not include SNPs in *WWC1* (*KIBRA*) or *CTNNBL1* (Liu *et al.* [under review]), suggesting that the analyzed traits are not significantly influenced by SNPs in these genes in our study population. The three most significant findings showed ~~association~~ P-values at or below $1x10^{-7}$ and were observed with SNPs rs9882688 ($P = 7.8x10^{-9}$ on chr 3p21.32) for trait "WL_save" (part of the CERAD cognitive battery measuring the proportion of learned words vs. recalled words), with rs1016365 ($P = 9.7x10^{-8}$ on chr 8q13.3) for "ItemItem" (associative episodic memory task where probands were asked to learn and recall words irrespective of their pairing with other words), and with rs113948889 ($P = 9.9x10^{-8}$ on chr 12p13.33) for "TFEUWC" (a spatial working memory paradigm combined with tasks testing frontal executive control; s~~S~~ee Supplementary Material for more information on these and all remaining traits). All of these signals were flanked by multiple additional SNPs showing ~~association~~ P-values at or below $1x10^{-5}$ indicating that they do not reflect technical artifacts (see Supplementary Figure 2-4 for Manhattan and Q-Q plots for GWAS results of these three traits). Only the signal with rs9882688 on chr 3 surpassed the threshold for genome-wide significance (i.e. P-values at or below $5x10^{-8}$, a ~~value~~ cutoff frequently used in the context of GWAS, see McCarthy *et al.* 2008). This SNP, which itself does not map to any known open reading frame, is located approx. 20kb upstream from the 5' end of miRNA hsa-mir-138-1 and, thus, potentially within active upstream regulatory elements of this miRNA. This interpretation is supported by the fact that rs9882688 is located within an ENCODE DNase I hypersensitivity cluster and within a known H3K27Ac mark, two features typically characterizing active regulatory elements (ENCODE Project Consortium *et al.* 2012). The second leading GWAS signal was elicited by SNP rs1016365, which is located approx. 6 kb 3' of *EYA1* (Homo sapiens eyes absent homolog 1 [Drosophila]) a member of the eyes absent (EYA) family of proteins. The third best associated SNP in our GWAS (rs113948889) maps to an intron of *DCP1B* (encoding decapping mRNA 1B), which is a core component of the mRNA decapping complex, a key factor in the regulation of mRNA decay. Focusing on these top GWAS findings, we next performed a number of different *in silico* and *in vitro* experiments to assess their potential role on miRNA function.

### 3.2. *In silico* predictions of miRNA-to-mRNA binding and potential SNP effects.

Using a bioinformatic tool recently developed in our group (Schilling 2011, Schilling 2013), we predicted the potential role of the GWAS SNPs on chr 3p21.32, 8q13.3, and 12p13.33 (and their proxies, i.e. other SNPs in strong LD [$r^2 \geq 0.5$] and mapping within ±1 Mb) on their potential to interfere with miRNA-to-mRNA binding. These analyses did not identify any such effects for the GWAS signals on chr 3 or 8, but several potentially relevant predictions for the memory associated SNPs on chr 12p13.33 (Table 1). All of the SNPs predicted to interfere with miRNA binding were proxies of rs113948889 with $r^2$ values of 1 and suggested a potential up-regulation of protein expression conferred by the respective non-reference

alleles. The strongest effect was estimated for rs112215626, predicted to interfere with the binding of hsa-miR-4775 to the 3'UTR of *DCP1B* mRNA (see miRNA-to-mRNA alignment in Figure 1a). The second strongest effect was estimated for rs1044950, which was predicted to interfere with the binding of hsa-miR-138-5p to the 3' UTR of another *DCP1B* transcript (Figure 1b). Interestingly, the same SNP is located within the coding sequence of alternative *DCP1B* transcripts where it is predicted to elicit an amino acid change from alanine to valine at the respective residues (i.e. Ala273Val, Ala249Val, Ala375Val; Supplementary Table 2). However, this missense substitution is not predicted to significantly alter protein function in any of the affected *DCP1B* transcripts (Supplementary Table ~~2~~3) *in silico* based on estimates from PolyPhen2 (Adzhubei *et al.* 2010) or SIFT (URL: http://sift.bii.a-star.edu.sg/), indicating that the presumed effects on miRNA-to-mRNA binding may represent the overarching functional mechanism underlying the GWAS signal at this locus. Hence, we selected to follow-up the two leading potential *DCP1B* miRNA SNPs (i.e. rs112215626 and rs1044950) *in vitro*.

### 3.3. *In vitro* assessment of SNPs predicted to affect miRNA-to-mRNA binding.

We conducted luciferase reporter assays in naïve HEK293 cells and SH-SY5Y cells using two different 3'UTR constructs (containing either the reference or non-reference alleles) of *DCP1B* transcripts ENST00000540622 and ENST00000541700 predicted to bind hsa-mir-138-5p and hsa-mir-4775, respectively. In HEK293 cells, co-transfections of the resulting 3'UTR *Renilla* vectors and hsa-mir-138-5p showed significant reductions of luciferase luminescence in comparison to co-transfections with the non-binding miRNA control ($P_{one\text{-}tailed} \leq 0.000191$), confirming our predictions that this miRNA binds to the corresponding 3'UTR *in vitro* (Figure 2a). Analyses comparing luciferase luminescence with respect to allele status at rs1044950 revealed a consistent and significant increase in normalized luciferase expression in constructs containing the minor A-allele ($n = 7$, $P = 0.0470$; Figure 2a). While co-transfection of the same reporter constructs with hsa-mir-138-5p to SH-SY5Y cells generally showed similar effects pointing in the same direction, the difference in luciferase expression between constructs containing the G- vs. A-allele was not statistically significant ($n = 9$, $P = 0.0866$, Figure 2a). Thus, in both cell lines the non-reference (minor) A-allele of SNP rs1044950 increased luciferase expression as compared to the reference (major) G-allele by 11.8% (HEK293) and 10.5% (SH-SY5Y). These findings are in line with our *in silico* predictions, which suggested stronger binding of hsa-mir-138-5p in 3'UTR sequences containing the reference (G) allele compared to the alternative (A) allele. In contrast, we did not observe a significant reduction of *Renilla* expression upon co-transfecting either reporter construct containing *DCP1B* transcript ENST00000540622 with SNP rs112215626 and hsa-mir-4775 compared to the non-binding miRNA in control experiments in neither HEK293 nor SH-SY5Y cells ($n = 7$ and 6, respectively, $P_{one\text{-}tailed} \geq 0.05$, Figure 2b). This suggests that this miRNA, as opposed to hsa-mir-138-5p, does not bind to the corresponding *DCP1B* transcript, at least under these experimental conditions. In summary, the results of the luciferase reporter experiments suggest that SNP rs1044950 elicits allele-specific effects on the expression of constructs containing the corresponding *DCP1B* 3'UTR in the presence of hsa-mir-138-5p *in vitro*.

### 3.4. Analysis of expression levels of hsa-mir-138-5p and *DCP1B* mRNA in human post-mortem brain tissue.

While both hsa-mir-138-1 (Landgraf *et al.* 2007) and transcripts of *DCP1B* (URL: http://human.brain-map.org/) were previously shown to be expressed in both hippocampus and frontal cortex in humans, no data exist as to whether this expression actually occurs at the same time, a prerequisite condition for the interaction effects observed *in vitro* to also be relevant *in vivo*. To address this question, we obtained three different post-mortem hippocampus and frontal cortex specimen, which were profiled for both miRNA and mRNA expression patterns. qPCR of hsa-mir-138-5p revealed high expression of this miRNA in both hippocampal and frontal brain slices for all three individuals (Figure 3a). Hsa-mir-138-5p expression levels were comparable to those observed for hsa-miR-let-7b, a miRNA ubiquitously expressed in many human tissues including brain (and used here as positive control miRNA), in the same specimen (data not shown). Semi-quantitative PCR of *DCP1B* mRNA in the same brain samples revealed a more variable expression pattern (Figure 3b). Using this method *DCP1B* mRNA was only detectable in two of the three human brain samples (probands 2 and 3 in Figure 3b). Further, in both of these probands *DCP1B* mRNA expression levels were higher in frontal cortex as compared to hippocampus (owing to the semi-quantitative nature of the experiments, these differences could not be assessed for statistical significance). Regardless of the observed interindividual and regional expression differences, these experiments clearly demonstrate that both hsa-mir-138-5p and *DCP1B* mRNA are co-expressed simultaneously in both the hippocampi and frontal cortices in human brain, setting the temporal and spatial stage for an interaction of these two RNA molecules *in vivo*.

### 3.5. Expression quantitative trait locus (eQTL) analyses of hsa-mir-138-5p using next-generation sequencing data.

Although the lead GWAS signal (elicited by rs9882688) identified in this study was not predicted to interfere with miRNA-to-mRNA binding *in silico*, this SNP maps into a potential regulatory site 20kb upstream of miRNA hsa-mir-138-1. The primary transcript of this miRNA is processed into two different mature products hsa-mir-138-5p and hsa-mir-138-1-3p, which are both expressed in humans (Landgraf *et al.* 2007). Notably, hsa-mir-138-5p is the same miRNA whose binding to *DCP1B* is also potentially affected by the presence of SNP rs1044950, as suggested by the *in silico* and *in vitro* experiments outlined above. Thus, a potential effect of rs9882688 on the expression of hsa-mir-138-5p could be indicative of a more systematic involvement of this miRNA in human memory performance. To this end, we performed eQTL analyses on NGS-based small-RNA sequencing data in over 300 human lymphoblastoid cell line ~~(LCL)~~ samples from the GEUVADIS project (Lappalainen et al. 2013). The results of these analyses revealed a significant dose-dependent effect of this SNP on hsa-mir-138-5p expression in these peripheral cell lines. Specifically, the presence of the minor G-allele of rs9882688 was associated with increased hsa-miR-138-5p expression levels (n = 309, beta = 80.87, standard error [SE] = 23.00, P-value = 0.000504, Figure 4). This finding was not solely driven by the two G-allele homozygotes in this dataset as evidenced by eQTL results after exclusion of these individuals (n = 307, beta = 77.35, SE = 25.56, P = 0.00270). These data suggest that the same SNP showing association with episodic memory

performance in humans, also significantly correlates with changes in hsa-mir-138-5p expression in human peripheral cell lines.

## 4. Discussion

We investigated the potential role of common DNA sequence variants associated with human memory performance in miRNA-mediated regulation of gene expression. A GWAS analysis on 13 memory traits in up to 1,318 individuals aged 60 years or older revealed a number of potential association signals in both working ("TFEUWC" with rs113948889) and episodic memory ("WL_SAVE" with rs9882688 and "ItemItem" with rs1016365) domains. Among these were SNPs predicted to be involved in the expression and function of hsa-mir-138-5p, a miRNA known to be important in brain development and function. Specifically, genotypes at SNP rs9882688 (which represented the lead memory GWAS signal in this study) were shown to correlate significantly with the expression of this hsa-mir-138-5p in human LCLs lymphoblastoid cell lines using next-generation small-RNA sequencing data collected as part of the GEUVADIS project. In addition, we found that SNP rs1044950 (as proxy of another top memory-associated GWAS signal) leads to allele-specific changes in the expression of reporter constructs containing the 3'UTR sequence of *DCP1B* transcripts predicted to contain binding sites for hsa-mir-138-5p in both peripheral (HEK293, P = 0.047) and neuronal (SH-SY5Y, P = 0.0866) human cell lines. Finally, expression profiling of both hsa-mir-138-5p and *DCP1B* mRNA in post-mortem human frontal cortex and hippocampus brain tissue revealed that both putative interactants are co-expressed in brainthe same tissue at the same time. In summary, in this study various lines of independent evidence (i.e. genetic, functional, gene expression) converge on the notion that hsa-mir-138-5p may play a significant role in processes related to human episodic memory performance.

The data from our study are in line with previous research on the potential role of mir-138 in mammalian brain function. For instance, Miska (Miska *et al.* 2004) showed that mir-138 expression levels increase with age in the developing rat brain reaching their peak in juvenile and adult rats. Landgraf (Landgraf *et al.* 2007) later showed that mir-138 was also highly expressed in adult human brain samples, including frontal cortex and hippocampus. More recently, mir-138 was identified as part of a functional screen for dendritic miRNAs that regulate spine morphogenesis in rats (Siegel *et al.* 2009). In that study, mir-138 was found to act as a negative regulator of dendritic spine size possibly by tuning the activity of antagonistic signaling pathways (e.g. those regulated by rat acyl protein thioesterase 1 [APT1]) that regulate the actin cytoskeleton in spines. In a review on the same topic Schratt hypothesized that "Given the crucial role of the spine actin cytoskeleton in long-term potentiation, it is tempting to speculate that activity-dependent regulation of these miR-138RNA-related pathways might also contribute to long-lasting forms of synaptic plasticity [...]" (Schratt 2009). Our data, in which we observed multiple converging lines of genetic evidence suggesting a potential role of hsa-mir-138-5p in episodic memory performance, provide some first independent support of this hypothesis and extend it to humans. In addition to *DCP1B*, hsa-mir-138-5p is predicted to target a large number of different human transcripts *in silico* (ranging between a few hundreds to a few thousands depending on the prediction algorithm used). In the GWAS results generated here, genes containing hsa-mir-138-5p targets identified by three or more of the prediction algorithms show a significant ($P < 0.05$ based on 100,000 permutations) enrichment for memory-associated SNPs as compared to genes not targeted by this miRNA (Supplementary Table 4X), further supporting the notion that hsa-mir-138-5p represents a potential molecular regulator of human memory function.

The gene *DCP1B* encodes "decapping mRNA 1B" which is a core component of the mRNA decapping complex, a key factor in the regulation of mRNA decay. Decapping and mRNA degradation takes places in P-bodies (processing bodies), cytoplasmic foci visible by light microscopy in somatic cells of vertebrates and other organisms (Kulkarni *et al.* 2010). Importantly, P-bodies have been suggested to be one of the predominant sites of miRNA-mediated mRNA degradation, a process that is inhibited upon depletion of the decapping DCP1:DCP2 complex (Behm-Ansmant *et al.* 2006). Thus, *DCP1B* and mir-138 function within the same general pathway, i.e. the degradation of mRNAs bound by miRNAs, likely including those targeted by hsa-mir-138 itself.

While the novel experimental data generated as part of this projecthere support the hypothesis that hsa-mir-138-5p plays an important role in physiological mechanisms involved in human memory performance, we note the following potential limitations of that need be considered when interpreting our findings. First and foremost, the functional genetic experiments implying a role of rs1044950 in interfering with miRNA-to-mRNA binding are based on *in vitro* experiments using reporter constructs. While it is tempting to speculate that these effects are also relevant *in vivo*, no direct experimental proof of this interpretation currently exists. In humans, however, this type of evidence is difficult to come by owing to the fact that molecular mechanisms in the living human brain cannot be monitored at sufficient resolution with current technologies. In order for the hypothesized effects to take place *in vivo*, both interactants need to be co-expressed in the same tissue at the same time. Our RNA-profiling experiments using human frontal cortex and hippocampus samples clearly demonstrate that this is the case for hsa-mir-138-5p and *DCP1B*. Second, another major conclusion of this study is that memory-associated SNP rs9882688 is involved in the regulation of hsa-mir-138-5p expression. While this could be shown in LCLs lymphoblastoid cell lines, it remains unclear whether these effects are also relevant in human brain. This question could be addressed by genotyping and miRNA profiling a sufficiently large collection of small-RNA extracts from post-mortem human brain tissue (e.g. n~300, similar to the LCL sample size used here), a data set currently not available to us. Third, linking the GWAS results for rs9882688 to this SNP's eQTL effects on hsa-mir-138-5p suggests that the same (i.e. G) allele increasing miRNA expression is associated with worse episodic memory performance (indicated by the negative beta-coefficient in Supplementary Table 1). Increased miRNA abundance is typically interpreted to lead to an increase in mRNA target repression and, as a consequence, reduced target gene expression. For SNP rs1044950, however, the minor (A) allele, associated with worse memory performance, leads to a decrease in miRNA-to-mRNA binding *in vitro*. This latter finding would suggest an increased target gene expression, i.e. an effect opposite to what can be expected from the eQTL results with rs9882688. One possible explanation for these different effect directions is the involvement of competing endogenous RNAs (ceRNAs). Such ceRNAs were recently proposed to exist, e.g. generated from transcribed pseudogenes, long noncoding RNAs, or stable RNAs (Salmena *et al.* 2011, Helwak *et al.* 2013). Here they could lead to increased levels of hsa-mir-138-5p in A-allele carriers of rs1044950, i.e. similar to what is observed for rs9882688-G. Finally, it needs to be emphasized that the GWAS results reported here represent preliminary findings that need to be replicated in independent data sets. However, even if these were to reveal

smaller effect estimates than those reported here (~~a situation not uncommon in the context of genetic association findings and often referred to as the~~e.g. as a result of the "winner's curse ~~phenomenon~~"; Kraft 2008), this should have no bearing on the functional genetic and expression profiling results of our study. In addition to generating independent genetic association data, future work will need to extend our eQTL findings to the CNS, confirm the regulatory role of hsa-mir-138-5p on endogenous expression of *DCP1B* and other target genes and their corresponding proteins (in particular those potentially involved in human memory function, such as *WWC1* [*KIBRA*]), and assess the role of this miRNA on their putative targets *in vivo*.

In summary, by combining unbiased genome-wide screening with extensive *in silico* modeling, *in vitro* functional assays, and gene expression profiling, our study identified hsa-mir-138-5p as a potential molecular regulator of human memory function. Future work is needed to assess the relevance of these findings *in vivo* and to explore other regulators and targets of this highly abundant miRNA, in particular their connection to memory and other cognitive domains.

**Acknowledgements**

This work is supported by the German Federal Ministry of education and Research (BMBF [grants #16SV5536K, #16SV5537, #16SV5538, and #16SV5837; previously #01UW0808]), the Max Planck Society, and a Gottfried Wilhelm Leibniz Award of the German Research Foundation to UL. J.S. and S.A. were supported by fellowships of the Max Planck International Research Network on Aging (MaxNetAging).

## References


Abecasis, G.R., Altshuler, D., Auton, A., Brooks, L.D., Durbin, R.M., Gibbs, R.A., Hurles, M.E., McVean, G.A. (2010). A map of human genome variation from population-scale sequencing. Nature 467 (7319), 1061-73.

Adzhubei, I.A., Schmidt, S., Peshkin, L., Ramensky, V.E., Gerasimova, A., Bork, P., Kondrashov, A.S., Sunyaev, S.R. (2010). A method and server for predicting damaging missense mutations. Nat Methods 7 (4), 248-9.

Behm-Ansmant, I., Rehwinkel, J., Doerks, T., Stark, A., Bork, P., Izaurralde, E. (2006). mRNA degradation by miRNAs and GW182 requires both CCR4:NOT deadenylase and DCP1:DCP2 decapping complexes. Genes Dev 20 (14), 1885-98.

Bertram, L., Böckenhoff, A., Demuth, I., Düzel, S., Eckardt, R., Li, S.C., Lindenberger, U., Pawelec, G., Siedler, T., Wagner, G.G., Steinhagen-Thiessen, E. (2013). Cohort profile: The Berlin Aging Study II (BASE-II). Int J Epidemiol.

Betel, D., Koppal, A., Agius, P., Sander, C., Leslie, C. (2010). Comprehensive modeling of microRNA targets predicts functional non-conserved and non-canonical sites. Genome Biol 11 (8), R90.

ENCODE Project Consortium, Bernstein, B.E., Birney, E., Dunham, I., Green, E.D., Gunter, C., Snyder, M. (2012). An integrated encyclopedia of DNA elements in the human genome. Nature 489 (7414), 57-74.

Fillenbaum, G.G., van Belle, G., Morris, J.C., Mohs, R.C., Mirra, S.S., Davis, P.C., Tariot, P.N., Silverman, J.M., Clark, C.M., Welsh-Bohmer, K.A., Heyman, A. (2008). Consortium to Establish a Registry for Alzheimer's Disease (CERAD): The first twenty years. Alzheimers Dement 4 (2), 96-109.

Goldberg Hermo, X., Lemos Giráldez, S., Fañanás Saura, L. (2014). A systematic review of the complex organization of human cognitive domains and their heritability. Psicothema 26 (1), 1-9.

Griffiths-Jones, S., Grocock, R.J., van Dongen, S., Bateman, A., Enright, A.J. (2006). miRBase: microRNA sequences, targets and gene nomenclature. Nucleic Acids Res 34 (Database issue), D140-4.

Helwak, A., Kudla, G., Dudnakova, T., Tollervey, D. (2013). Mapping the Human miRNA Interactome by CLASH Reveals Frequent Noncanonical Binding. Cell 153 (3), 654-65.

Kraft, P. (2008). Curses--winner's and otherwise--in genetic epidemiology. Epidemiology 19 (5), 649-51; discussion 657-8.

Kulkarni, M., Ozgur, S., Stoecklin, G. (2010). On track with P-bodies. Biochem Soc Trans 38 (Pt 1), 242-51.

Landgraf, P., Rusu, M., Sheridan, R., Sewer, A., Iovino, N., Aravin, A., Pfeffer, S., Rice, A., Kamphorst, A.O., Landthaler, M., Lin, C., Socci, N.D., Hermida, L., Fulci, V., Chiaretti, S., Foà, R., Schliwka, J., Fuchs, U., Novosel, A., Müller, R.U., Schermer, B., Bissels, U., Inman, J., Phan, Q., Chien, M., Weir, D.B., Choksi, R., De Vita, G., Frezzetti, D., Trompeter, H.I., Hornung, V., Teng, G., Hartmann, G., Palkovits, M., Di Lauro, R., Wernet, P., Macino, G., Rogler, C.E., Nagle, J.W., Ju, J., Papavasiliou, F.N., Benzing, T., Lichter, P., Tam, W., Brownstein, M.J., Bosio, A., Borkhardt, A., Russo, J.J., Sander, C., Zavolan, M., Tuschl, T. (2007). A Mammalian microRNA Expression Atlas Based on Small RNA Library Sequencing. Cell 129 (7), 1401-14.

602 Lappalainen, T., Sammeth, M., Friedländer, M.R., ´t Hoen, P.A., Monlong, J., Rivas, M.A.,
603 Gonzàlez-Porta, M., Kurbatova, N., Griebel, T., Ferreira, P.G., Barann, M., Wieland, T.,
604 Greger, L., Van Iterson, M., Almlöf, J., Ribeca, P., Pulyakhina, I., Esser, D., Giger, T.,
605 Tikhonov, A., Sultan, M., Bertier, G., Macarthur, D.G., Lek, M., Lizano, E., Buermans,
606 H.P., Padioleau, I., Schwarzmayr, T., Karlberg, O., Ongen, H., Kilpinen, H., Beltran, S.,
607 Gut, M., Kahlem, K., Amstislavskiy, V., Stegle, O., Pirinen, M., Montgomery, S.B.,
608 Donnelly, P., McCarthy, M.I., Flicek, P., Strom, T.M., Geuvadis, C., Lehrach, H., Schreiber,
609 S., Sudbrak, R., Carracedo, A., Antonarakis, S.E., Häsler, R., Syvänen, A.C., van Ommen,
610 G.J., Brazma, A., Meitinger, T., Rosenstiel, P., Guigó, R., Gut, I.G., Estivill, X.,
611 Dermitzakis, E.T., Geuvadis, C. (2013). Transcriptome and genome sequencing uncovers
612 functional variation in humans. Nature 501 (7468), 506-11.
613 Li, S.C., Papenberg, G., Nagel, I.E., Preuschhof, C., Schröder, J., Nietfeld, W., Bertram, L.,
614 Heekeren, H.R., Lindenberger, U. Bäckman, L. (2013). Aging magnifies the effects of
615 dopamine transporter and D2 receptor genes on backward serial memory. Neurobiol Aging
616 34 (1) 358 e1-10.
617 Lill, C.M., Schilling, M., Ansaloni, S., Schröder, J., Jaedicke, M., Luessi, F., Schjeide, B.M.,
618 Mashychev, A., Graetz, C., Akkad, D.A., Gerdes, L.A., Kroner, A., Blaschke, P., Hoffjan,
619 S., Winkelmann, A., Dörner, T., Rieckmann, P., Steinhagen-Thiessen, E., Lindenberger, U.,
620 Chan, A., Hartung, H.P., Aktas, O., Lohse, P., Buttmann, M., Kümpfel, T., Kubisch, C.,
621 Zettl, U.K., Epplen, J.T., Zipp, F., Bertram, L. (2014). Assessment of microRNA-related
622 SNP effects in the 3' untranslated region of the *IL22RA2* risk locus in multiple sclerosis.
623 Neurogenetics. DOI 10.1007/s10048-014-0396-y
624 Lindenberger, U., Nagel, I.E., Chicherio, C., Li, S.C., Heekeren, H.R., Bäckman, L. (2008).
625 Age-related decline in brain resources modulates genetic effects on cognitive functioning.
626 Front Neurosci 15;2 (2), 234-44.
627 Liu, T., Li, S.C., Papenberg, G., Schröder, J., Roehr, J.T., Nietfeld, W., Lindenberger, U.,
628 Bertram, L. (2014) No Association between CTNNBL1 and Episodic Memory Performance.
629 Under review.
630 Marchini, J., Howie, B. (2010). Genotype imputation for genome-wide association studies.
631 Nat Rev Genet 11 (7), 499-511.
632 McCarthy, M.I., Abecasis, G.R., Cardon, L.R., Goldstein, D.B., Little, J., Ioannidis, J.P.,
633 Hirschhorn, J.N. (2008). Genome-wide association studies for complex traits: consensus,
634 uncertainty and challenges. Nat Rev Genet 9 (5), 356-69.
635 McClearn, G.E., Johansson, B., Berg, S., Pedersen, N.L., Ahern, F., Petrill, S.A., Plomin, R.
636 (1997). Substantial Genetic Influence on Cognitive Abilities in Twins 80 or More Years
637 Old. Science 276 (5318), 1560-3.
638 Milnik, A., Heck, A., Vogler, C., Heinze, H.J., de Quervain, D.J., Papassotiropoulos,
639 A.,(2012). Association of *KIBRA* With Episodic and Working Memory: A Meta-Analysis.
640 Am J Med Genet B Neuropsychiatr Genet 159B (8), 958-69.
641 Miska, E.A., Alvarez-Saavedra, E., Townsend, M., Yoshii, A., Šestan, N., Rakic, P.,
642 Constantine-Paton, M., Horvitz, H.R. (2004). Microarray analysis of microRNA expression
643 in the developing mammalian brain. Genome Biol 5 (9), R68.
644 Morris, J.C., Heyman, A., Mohs, R.C., Hughes, J.P., van Belle, G., Fillenbaum, G., Mellits,
645 E.D., Clark, C. (1989). The Consortium to Establish a Registry for Alzheimer's Disease

(CERAD). Part I. Clinical and neuropsychological assessment of Alzheimer's disease. Neurology 39 (9), 1159-65.

Papassotiropoulos, A., de Quervain, D.J. (2011). Genetics of human episodic memory: dealing with complexity. Trends Cogn Sci 15 (9), 381-7.

Papassotiropoulos, A., Stephan, D.A., Huentelman, M.J., Hoerndli, F.J., Craig, D.W., Pearson, J.V., Huynh, K.D., Brunner, F., Corneveaux, J., Osborne, D., Wollmer, M.A., Aerni, A., Coluccia, D., Hänggi, J., Mondadori, C.R., Buchmann, A., Reiman, E.M., Caselli, R.J., Henke, K., De Quervain, D.J. (2006). Common *Kibra* Alleles Are Associated with Human Memory Performance. Science 314 (5798), 475-8.

Papenberg, G., Li, S.C., Nagel, I.E., Nietfeld, W., Schjeide, B.M., Schröder, J., Bertram, L., Heekeren, H.R., Lindenberger, U., Bäckman, L. (2014). Dopamine and glutamate receptor genes interactively influence episodic memory in old age. Neurobiol Aging 35 (5), 1213 e3-8

Peterson, S.M., Thompson, J.A., Ufkin, M.L., Sathyanarayana, P., Liaw, L., Congdon, C.B. (2014). Common features of microRNA target prediction tools. Front Genet 5, 23.

Salmena, L., Poliseno, L., Tay, Y., Kats, L., Pandolfi, P.P. (2011). A ceRNA Hypothesis: The Rosetta Stone of a Hidden RNA Language? Cell 146 (3), 353-8.

Satoh, J. (2012). Molecular network of microRNA targets in Alzheimer's disease brains. Exp Neurol 235 (2), 436-46.

Schilling M. (2011). *In silico* assessment of the effects of single nucleotide polymorphisms on miRNA-mRNA interactions. Bachelor’s thesis. Department of Mathematics and Computer Science – FU Berlin, Berlin, Germany.

Schilling M. (2013). The role of DNA sequence variants predicted to alter miRNA-mRNA interactions in disease pathogenesis. Master’s thesis. Department of Mathematics and Computer Science – FU Berlin, Berlin, Germany.

Schratt, G. (2009). microRNAs at the synapse. Nat Rev Neurosci 10 (12), 842-9.

Siegel, G., Obernosterer, G., Fiore, R., Oehmen, M., Bicker, S., Christensen, M., Khudayberdiev, S., Leuschner, P.F., Busch, C.J., Kane, C., Hübel, K., Dekker, F., Hedberg, C., Rengarajan, B., Drepper, C., Waldmann, H., Kauppinen, S., Greenberg, M.E., Draguhn, A., Rehmsmeier, M., Martinez, J., Schratt, G.M. (2009). A functional screen implicates microRNA-138-dependent regulation of the depalmitoylation enzyme APT1 in dendritic spine morphogenesis. Nat Cell Biol 11 (6), 705-16.

Welter, D., MacArthur, J., Morales, J., Burdett, T., Hall, P., Junkins, H., Klemm, A., Flicek, P., Manolio, T., Hindorff, L., Parkinson, H. (2014). The NHGRI GWAS Catalog, a curated resource of SNP-trait associations. Nucleic Acids Res 42 (Database issue), D1001-6.

Zhang, L., Yang, S., Wennmann, D.O., Chen, Y., Kremerskothen, J., Dong, J. (2014). KIBRA: In the brain and beyond. Cell Signal 26 (7), 1392-1399.

683 **Figure Legends**

684

685 **Figure 1:** Predicted miRNA binding sites in the *DCP1B* transcripts. *(a)* Rs112215626 is
686 located in the seed region of hsa-miR-4775. The alternative (G) allele of rs112215626
687 (highlighted in red) may alter binding affinity of hsa-miR-4775 to the *DCP1B* 3'UTR and
688 therefore alter protein levels. *(b)* Rs1044950 is located in the seed region of hsa-miR-138-5p.
689 The alternative T allele of the rs1044950 (highlighted in red) may alter binding affinity of
690 hsa-miR-138-5p to the *DCP1B* 3'UTR and subsequently alter protein levels.
691

692 **Figure 2:** *In vitro* effects of rs1044950 and rs112215262 on miRNA-to-mRNA binding and
693 gene expression. The bar charts show the normalized *Renilla* luciferase expression in
694 constructs containing *DCP1B* 3'UTR and corresponding SNP alleles. Depicted are the mean
695 *Renilla* luciferase intensities and the standard errors relative to the control luciferase
696 intensities of the construct co-transfected with the non-targeting miRNA control
697 (corresponding to the horizontal line): *(a)* for transcript ENST00000541700 containing the
698 reference (G) or alternative (A) allele of rs1044950 and co-transfected with has-miR-138-5p
699 into HEK293 and SH-SY5Y cells. The relative mean luciferase luminescence of the construct
700 containing the G and the A allele was 0.585 (±0.0335) and 0.703 (±0.0417) in HEK293
701 cells, and 0.880 (±0.0256) and 0.985 (±0.0513) in SH-SY5Y cells. *(b)* for transcript
702 ENST00000540622 containing the reference (T) or alternative (C) allele of rs112215626 and
703 co-transfected with hsa-miR-4775 into HEK293 and SH-SY5Y cells. The relative mean
704 luciferase luminescence of the construct containing T and the C allele was 0.903 (±0.0692)
705 and 0.931 (±0.0382) in HEK293 cells, and 1.056 (±0.0582) and 1.041 (±0.0185) in SH-SY5Y
706 cells.
707

708 **Figure 3:** Expression profile of hsa-miR-138-5p and *DCP1B* in autopsy brain tissues of three
709 deceased human probands. *(a)* Amplification plot of qPCR experiments in three frontal
710 cortices (highlighted in purple) and three hippocampi (highlighted in green). Hsa-miR-138-5p
711 was expressed in both frontal cortex (FC) and hippocampus (HC; $C_T$ ~19). One of two NTCs
712 (non template control, highlighted in red) showed amplification at $C_T > 45$, where the other
713 one did not show any amplification. *(b)* Ethidium bromide stained gel electrophoresis in 1%
714 agarose displays the semi-quantitative levels of *DCP1B* cDNA (expected and observed at
715 ~850bp) in post-mortem human brain tissues. No expression was detected in proband 1 (P1).
716 The *DCP1B* cDNA levels were higher in the FC, compared to HC of proband 2 (P2) and
717 proband 3 (P3). A gDNA amplicon band (expected and observed at ~6.9kb) could be detected
718 and no band in the NTC.
719

720 **Figure 4:** Box plot of the distribution of hsa-miR-138-1-5p expression levels in
721 lymphoblastoid cell lines dependent on the rs9882688 genotype in 308 individuals of
722 European descent. Horizontal lines represent median values, boxes represent interquartile
723 ranges, and whiskers extend to 1.5x the interquartile range; values outside this range are
724 depicted as circles. Carriers of the rs9882688 G allele showed an increase in hsa-miR-138-1-
725 5p expression levels.

**Table 1: SNPs in LD with memory-associated SNP rs113948889 and predicted to affect miRNA-to-mRNA binding *in silico*.**

| GWAS SNP | miRNA target site SNP | CHR | BP | Distance to GWAS SNP | miRNA target site SNP | LD R2 | microRNA | Target gene | Target transcript |
|---|---|---|---|---|---|---|---|---|---|
| rs113948889 | rs112215626 | 12 | 2,059,337 | 44,833 | G/A | 1 | hsa-miR-4775 | DCP1B | ENST00000540622 |
| rs113948889 | rs1044950 | 12 | 2,061,982 | 42,188 | T/C | 1 | hsa-miR-138-5p | DCP1B | ENST00000541700 |
| rs113948889 | rs34730825 | 12 | 2,064,602 | 39,568 | C/T | 1 | hsa-miR-3147 | DCP1B | ENST00000543381 |
| rs113948889 | rs111963484 | 12 | 2,102,086 | 2,084 | C/A | 1 | hsa-miR-4270 | DCP1B | ENST00000535873 |
| rs113948889 | rs111963484 | 12 | 2,102,086 | 2,084 | C/A | 1 | hsa-miR-4441 | DCP1B | ENST00000535873 |
| rs113948889 | rs111963484 | 12 | 2,102,086 | 2,084 | C/A | 1 | hsa-miR-505-5p | DCP1B | ENST00000535873 |
| rs113948889 | rs112637373 | 12 | 2,102,271 | 1,899 | G/T | 1 | hsa-miR-2909 | DCP1B | ENST00000535873 |
| rs113948889 | rs34730825 | 12 | 2,064,602 | 39,568 | C/T | 1 | hsa-miR-92a-1-5p | DCP1B | ENST00000543381 |

Legend: Predicted miRNA target site SNPs in linkage disequilibrium with GWAS SNP rs113948889 listed in descending order of predicted effect on miRNA-to-mRNA binding. Minor alleles are listed first in "SNP allele" column. CHR = chromosome; BP = base-pair position on CHR; LD = linkage disequilibrium. Genomic annotations based on human genome (hg) build 19, transcript IDs according to ENSEMBL v.75. Shaded entries highlight SNPs assessed *in vitro*.

Figure 1.TIF


(a)
miRNA: hsa-miR-4775
mRNA: ENSG00000151065|ENST00000540622: rs112215626
miRNA 5' UUAAUUUUUUGUUUCGGUCACU 3'
mRNA 3' ...CAUUAAAAUAUUA-GUUAGGGA... 5'
miRNA 5' UUAAUUUUUUGUUUCGGUCACU 3'
mRNA 3' ...CGUUAAAAUAUUA-GUUAGGGA... 5'
(b)
miRNA: hsa-miR-138-5p
mRNA: ENSG00000151065|ENST00000541700: rs1044950
miRNA 5' AGCUGGUGUUGU-GAAUCAGGCCG 3'
mRNA 3' ...ACGACCACAUGAUCCCAGUGUGAA... 5'
miRNA 5' AGCUGGUGUUGU-GAAUCAGGCCG 3'
mRNA 3' ...AUGACCACAUGAUCCCAGUGUGAA... 5'

Figure 2.TIF

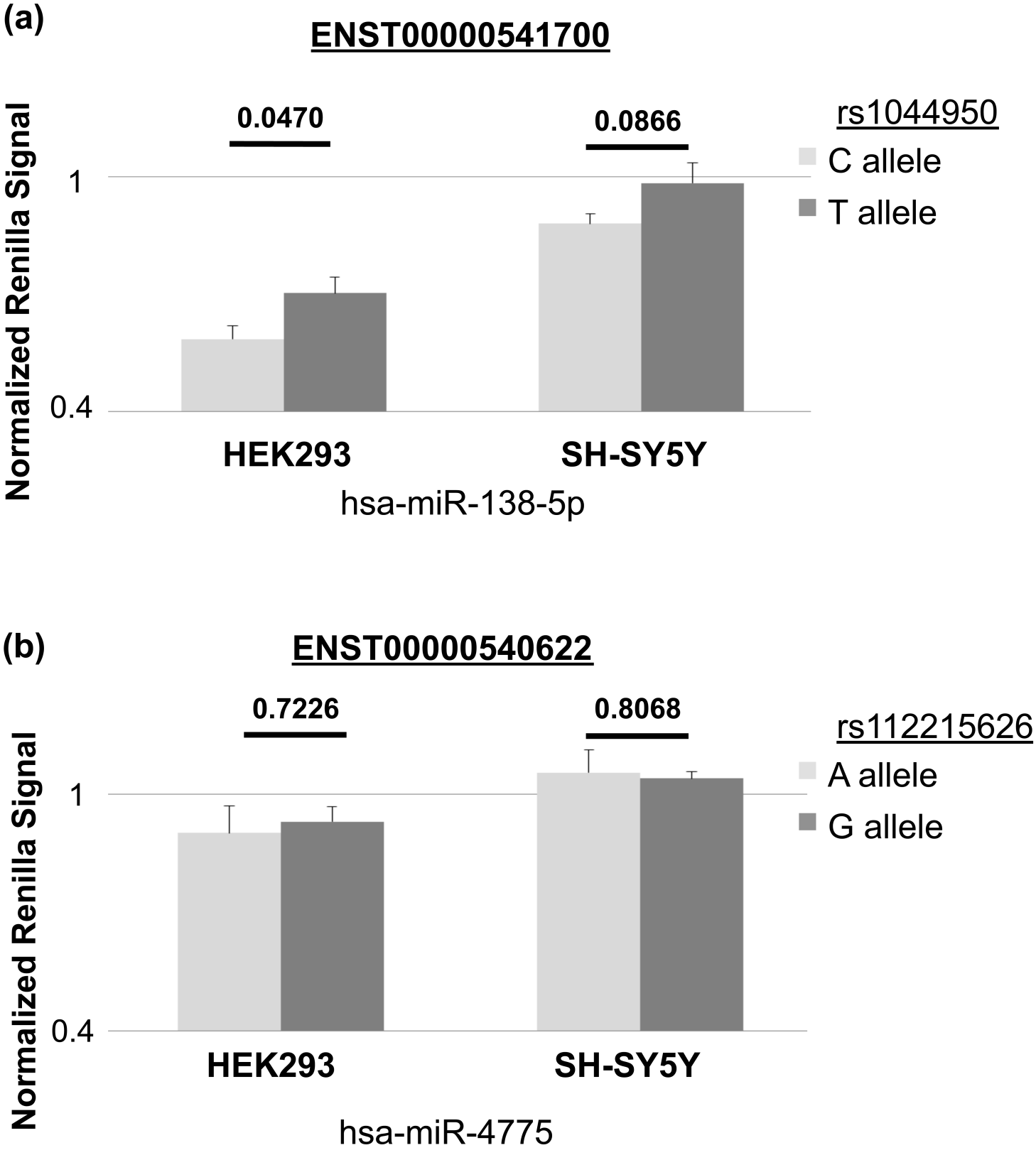
(a)
ENST00000541700
0.0470
0.0866
rs1044950
C allele
T allele
Normalized Renilla Signal
1
0.4
HEK293
SH-SY5Y
hsa-miR-138-5p
(b)
ENST00000540622
0.7226
0.8068
rs112215626
A allele
G allele
Normalized Renilla Signal
1
0.4
HEK293
SH-SY5Y
hsa-miR-4775

Figure 3.TIF

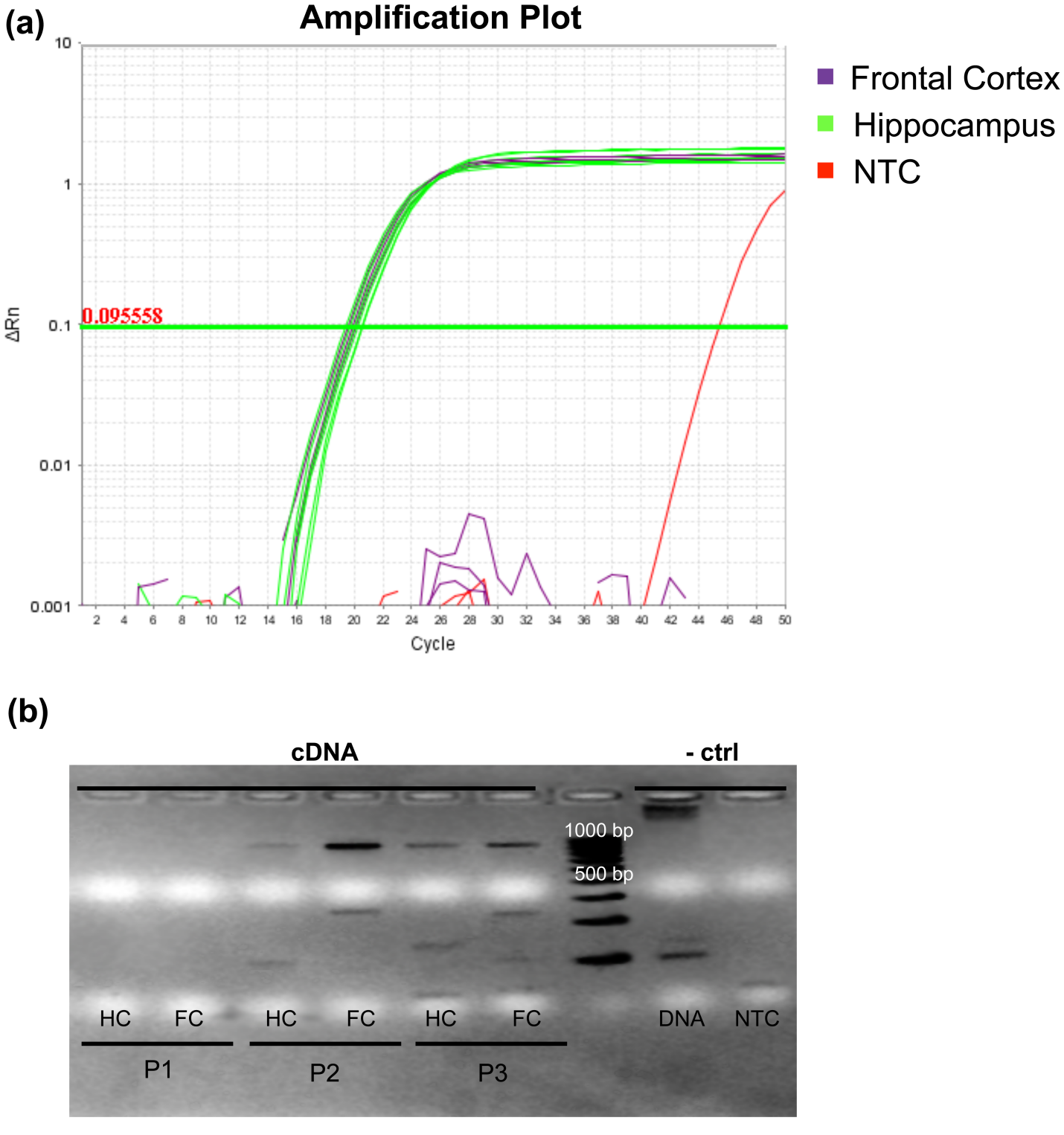
(a)
Amplification Plot
Frontal Cortex
Hippocampus
NTC
ΔRn
0.095558
Cycle
(b)
cDNA
- ctrl
1000 bp
500 bp
HC
FC
HC
FC
HC
FC
DNA
NTC
P1
P2
P3

Figure 4.TIF

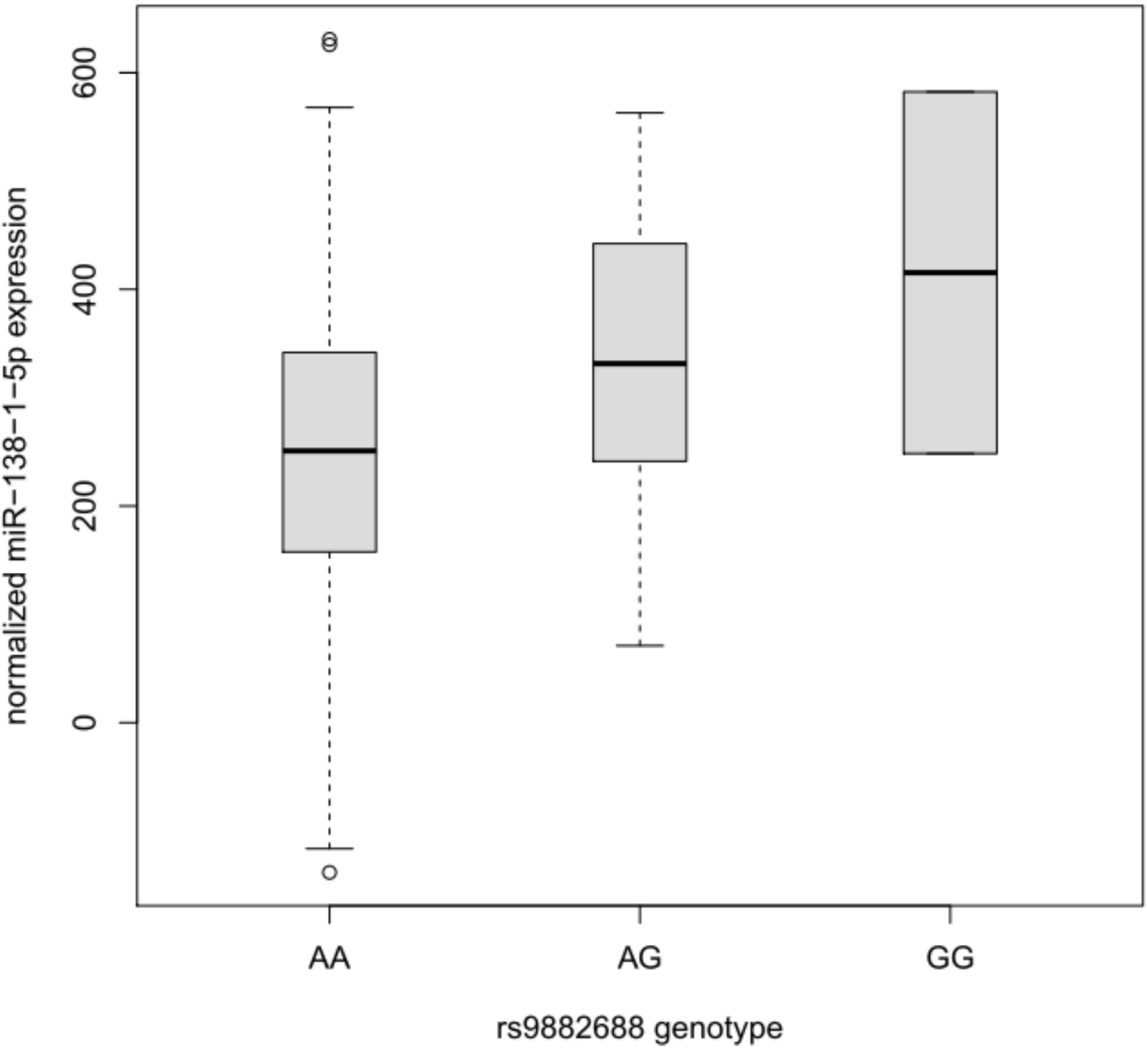
normalized miR−138−1−5p expression
0
200
400
600
AA
AG
GG
rs9882688 genotype